# Comparison and Application of Battery Modeling Methods for Conceptual Electric Aircraft

Jeshurun P. Horton,[1] Jeffryes W. Chapman,[2] and Mark K. Leader[3]
*NASA Glenn Research Center, Cleveland, OH, 44135, United States*

**Growing interest in design and optimization of electrified aircraft propulsion concepts prompts the need for accurate, flexible, and efficient methods to model battery systems. Presented in this paper are three battery modeling methods that have been used at NASA's Glenn Research Center, each representing different mathematical or electrical approaches. Thévenin equivalent circuit, normalization, and curve-fitting methods are compared against battery cell test data for the X-57 Maxwell electric aircraft technology demonstrator. The methods are then applied in a simple multidisciplinary optimization context using NASA's Six-Passenger Electric Quadrotor concept to determine their applicability and performance. The normalization method achieves the highest accuracy for steady and unsteady discharge rates with a voltage mean error percentage of 0.423% and 1.186%, respectively. Optimal quadrotor mission range between the models varies up to 0.5 nmi, identifying current battery modeling methods as a potentially significant contributor to mission analysis error. A set of relevant tools and techniques for conceptual battery modeling are identified in this paper, with conclusions made on the utility of each modeling approach for various design challenges.**

## I. Nomenclature

| | | |
|---|---|---|
| $A$ | = | exponential zone amplitude, Shepherd's equations (V) |
| $A_S$ | = | surface area (m$^2$) |
| $B$ | = | exponential zone time constant inverse, Shepherd's equations (A·h$^{-1}$) |
| $C$ | = | capacitance (F) |
| $C_p$ | = | heat capacity (J·deg C$^{-1}$) |
| $E_0$ | = | constant battery voltage, Shepherd's equations (V) |
| $F_V$ | = | cell normalized voltage |
| $h$ | = | convective heat transfer coefficient (W·m$^{-2}$·deg C$^{-1}$) |
| $I$ | = | current (A) |
| $K$ | = | polarization constant, Shepherd's equations (V·A$^{-1}$·h$^{-1}$) |
| kd | = | cell normalized discharge capacity |
| $k_{dI}$ | = | current parameter, Normalized discharge model (A$^{-1}$) |
| $k_{dT}$ | = | temperature parameter, Normalized discharge model (deg C$^{-1}$) |
| $k_{VT}$ | = | temperature parameter, Normalized discharge model (V·deg C$^{-1}$) |
| MPE | = | mean percent error |
| $Q$ | = | charge or discharge capacity (A·h) |
| $R$ | = | internal resistance (Ohm) |
| SOC | = | state-of-charge |
| $t$ | = | time (s) |
| $T$ | = | temperature (deg C) |

[1] Aerospace Engineer, Propulsion Systems Analysis Branch, jeshurun.p.horton@nasa.gov, AIAA Member.
[2] Aerospace Engineer, Propulsion Systems Analysis Branch, jeffryes.w.chapman@nasa.gov.
[3] Aerospace Engineer, Propulsion Systems Analysis Branch, mark.leader@nasa.gov, AIAA Member.

| | | |
|---|---|---|
| V | = | voltage (V) |
| ν | = | cell efficiency |
| τ | = | RC-circuit time constant (s) |

*Subscripts*

| | | |
|---|---|---|
| cell | = | battery cell |
| pack | = | battery pack |
| Line | = | battery circuit line |
| max | = | maximum (peak) |
| exp | = | exponential discharge zone |
| nom | = | nominal |
| oc, 0 | = | open-circuit |
| Th, 1 | = | Thévenin equivalent |
| amb | = | ambient |

## II. Introduction

Designing a battery system for an electric aircraft introduces a distinct set of challenges compared to an electric ground vehicle. Power and energy capacity requirements will influence the battery cell selection, cell count, electrical layout, cable sizing, thermal protections, and electrical safety protections, all of which affect the fixed empty weight, endurance, and maneuverability of the aircraft [1]. Stringent weight, thermal, and safety requirements for the aircraft push the battery design solution to be as minimal as possible while still meeting operational needs. This compels the use of multidisciplinary design analysis and optimization (MDAO) methods to capture the interactions between the battery system and other design disciplines. Accurate and quickly iterable battery modeling is required for such an MDAO process to be successful. While several battery modeling methods have been used at NASA's Glenn Research Center for these applications, there has been recent interest in selecting and enhancing one or more of these battery models to use for future electric aircraft concept designs.

Most battery models can be categorized as having electrochemical, mathematical, or electrical approaches [2]. Electrochemical models are generally the most complex and use knowledge of the chemical reactions occurring within the battery cell to estimate the overall performance [3]. These models, while very accurate, can be time-consuming to operate and require information that is not available for commercial batteries without extensive physical testing. Mathematical models are equation-based, and often use empirical or stochastic methods to capture battery trends [4]. These models are less complex to set up and can offer improved computational speeds, but are often designed for specific applications and can be less accurate if empirical relationships are used. Electrical models use an "equivalent circuit" to model battery behavior using a combination of voltage sources, resistors, inductors, and capacitors [5]. Electrical models can be further categorized into impedance models, Thévenin models, and runtime-based models. Electrical models tend to fall between electrochemical and mathematical models in terms of speed and accuracy. They can also be more effective at modeling non-linear changes in voltage due to current. A potential downside is that electrical models may require physical battery test data or assumptions to be made about the battery. This paper is not a comprehensive review of all battery modeling approaches, but rather focused on specific types of models in the mathematical and electrical categories.

Multiple factors must be considered when selecting a battery model for general conceptual MDAO applications. Ideally, the battery model should run fast enough to be included in a large-scale vehicle design without adding significant computational expense. The model should calculate cell-level performance with enough accuracy to produce the correct aircraft-level power requirements for a simulated mission. If desired, the model should contain external outputs such as heat loss and peak current that are necessary to design the aircraft's electrical, cooling, and safety systems. For notional conceptual designs, the model may be expected to work with easily obtainable or estimated battery cell data rather than depending on physical battery testing. The ideal model should ideally be adaptable to different cell types (e.g.: power cells and energy cells), and different cathode compositions (e.g.: NCA, NMC, LFP cells for lithium-ion). While lithium-ion batteries are the focus of this paper, it may be desired to extend the model's capability to other battery types, such as Lead-Acid and Ni-Mh. In some cases, battery charging speeds may be an early design consideration which would require a model that can simulate both charging and discharging sequences. The battery models examined in this study are each evaluated based on the above criteria.

Other considerations not included in this study, but important for specific modeling situations, are the effects of aging, capacity fade [6], over-discharge [7], cell faults [7], and overheating/thermal runaway [8]. In some cases, it may be desirable to extend the model from design to operational applications, such as representation of an aircraft using a "digital twin" system [9], or fault prediction using an onboard battery management system (BMS) [10], which would require additional modeling considerations.

Each of the models examined in this study have been used previously by NASA for multidisciplinary design [4, 5, 11]. The Equivalent Circuit model was used by Jeffrey Chin to model a nominal flight for the X-57 Maxwell demonstrator [5]. The Normalized model was developed by Wayne Johnson for the NASA Design and Analysis of Rotorcraft (NDARC) package [11], which is used by NASA's Revolutionary Vertical Lift Technology (RVLT) project for conceptual rotorcraft design. The Curve Fit model was developed by Edmond Wong, George Thomas, Mark Bell, and Jonathan Litt at NASA's Glenn Research Center for the Electrical Modeling and Thermal Analysis Toolbox (EMTAT) [12], a software toolkit for modeling electrified aircraft propulsion (EAP) systems.

Recent investment in the use of MDAO tools such as OpenMDAO [13] and Dymos [14] for conceptual design work has prompted the need for existing battery models to be built up in an integrated environment compatible with these new tools and optimization techniques. To accurately compare the battery models in terms of both accuracy and compatibility with a modern MDAO framework, the battery models are first assessed against available test data for a Samsung INR18650-30Q battery cell using MATLAB Simulink [15] to provide time-based input parameters. Next, the models are examined in a simple MDAO context using OpenMDAO and Dymos to model a dynamic mission for a fixed electric vertical takeoff and landing (eVTOL) vehicle design. NASA's Six-Passenger Quadrotor concept [16, 17] developed by the Revolutionary Vertical Lift Technology (RVLT) project is examined as a readily available example of an urban air mobility (UAM) concept for which battery performance modeling is a crucial element.

## III. Battery Modeling Methods

### A. Equivalent Circuit Model

The Equivalent Circuit model represents a battery cell as a Thévenin equivalent resistance-capacitance (RC) circuit shown in Fig. 1. This allows the performance states of the battery to be represented in terms of circuit resistance and capacitance. The model has been used for multiple concept studies, including past work on NASA's X-57 Maxwell electric aircraft [5].

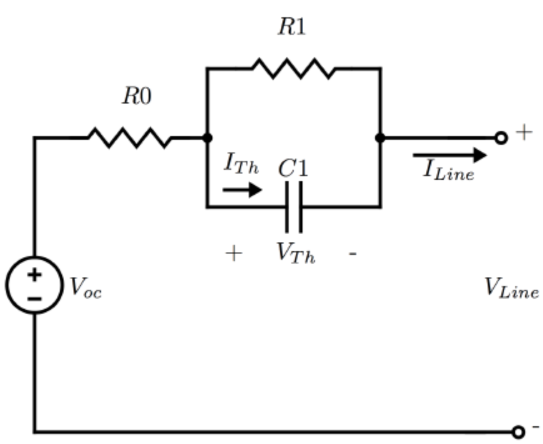


**Fig. 1 Thévenin equivalent Single RC circuit model. [5]**

**Fig. 2 Pulse discharge test setup. [5]**

The states in this model are open-circuit source voltage ($V_{oc}$), Thévenin equivalent voltage ($V_{Th}$), internal resistance ($R_0$), and the Thévenin equivalent resistance and capacitance ($R_{Th}$, $C_{Th}$). To represent a specific cell using this model, these parameters must be extracted from the battery across the full range of state-of-charge (SOC) and temperature the cell will be subject to. This is accomplished through a series of pulse discharge tests, where battery cells are placed in a temperature-controlled chamber and discharged over a given interval before being returned to equilibrium. The setup of one of these tests, conducted on 18650-30Q battery cells, is shown in Fig. 2. Displayed in Fig. 3 are the resulting pulse intervals (left), along with how each parameter is extracted from the pulse intervals for a measured SOC (right). Least-squares optimization is used to match values into a set of interpolation tables.

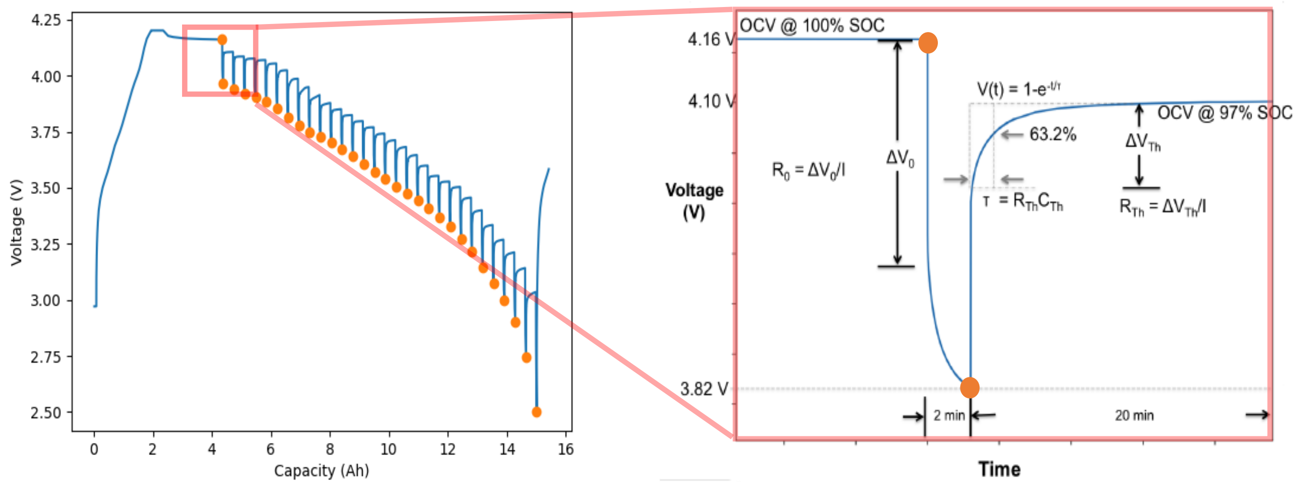


**Fig. 3 Parameter extraction from pulse discharge test. [5]**

When running the model, a given SOC and temperature are used to determine the value of $V_{oc}$, $R_0$, $R_{Th}$, and $C_{Th}$ from the interpolation table. $V_{Th}$ is determined by Eq. 1:

$$\frac{dV_{Th}}{dt} = \frac{I_{Line}}{C_{Th}} - \frac{V_{Th}}{R_{Th}C_{Th}} \tag{1}$$

The line voltage (cell voltage) is then computed by Eq. 2:

$$V_{Line} = V_{oc} - V_{Th} - I_{Line}R_0 \tag{2}$$

The model assumes there is no aging or capacity fade on the cell from prior use or from high discharge rates, meaning a battery lifecycle analysis would require further development. Due to the available range of the pulse discharge test, the model assumes the battery will not operate below 20% SOC. This is acceptable for most concept modeling cases, but additional testing would be needed to model scenarios such as emergency low-SOC battery usage.

As an electrical modeling approach, this method can be desirable for both speed and accuracy. The simplified circuit model paired with interpolation tables allows for fast computational speeds while capturing transient behavior, such as the inverse exponential gain to open-circuit voltage shown in Fig. 3 when current returns to zero. While the RC circuit is a simplified representation of an actual cell, the Equivalent Circuit model allows more RC "blocks" to be added modularly, resulting in higher precision at the cost of potentially reduced computational speed.

A limitation of the model is that pulse discharge test data is required to populate the interpolation tables, which is often not available for commercial batteries. While it is possible to approximate a new battery by discerningly scaling an existing battery's pulse discharge data, chemical differences will not be accurately captured which could lead to poor results. Another limitation is that accurately modeling battery charging using this approach requires a separate test, which was not performed for the battery cell examined in this study.

### B. Normalized Model

The approach taken for the NDARC software [11] battery model is to calibrate a set of parameterized equations based on available battery discharge data. Eqs. 3 and 4 for cell discharge contain the four parameters $k_{dI}$, $k_{dT}$, $R$, and $k_{VT}$ relating to the current and temperature response of the battery. These parameters are calibrated such that the normalized discharge curves overlap to form a single function known as $F_V(kd)$, where $kd$ corresponds to the cell discharge and $F_V$ corresponds to the cell voltage. Similar equations are applied to model battery charging.

$$kd = \frac{Q}{Q_{max}}(1 + k_{dI}I - k_{dT}(T_{cell} - T_{amb})) \tag{3}$$

$$F_V = (V + IR - k_{VT}(T_{cell} - T_{amb})^3)/V_{max} \tag{4}$$

The voltage for a given current, temperature, and discharge capacity can then be calculated with Eq. 5 by interpolating the table for $F_V$ and solving Eq. 4 for voltage:

$$V = V_{max}F_V + k_{VT}(T_{cell} - T_{amb})^3 - IR \tag{5}$$

The capacity used to compute $kd$ is determined from an adaptation of Peukert's capacity equation [18]. Fig. 4 shows a set of user input curves for a range of discharge rates (left), and the parameter-adjusted normalized curve from which points for the $F_V(kd)$ table are derived (right). Previously, the normalized function was generated by manually adjusting the four function parameters until the provided discharge dataset aligned closely. As part of this study, we developed an OpenMDAO tool to automatically generate the function by minimizing the cumulative RMSE value of the dataset using a sequential least squares programming (SLSQP) optimizer. This allows the model to be parameterized automatically, requiring only discharge data as an input.

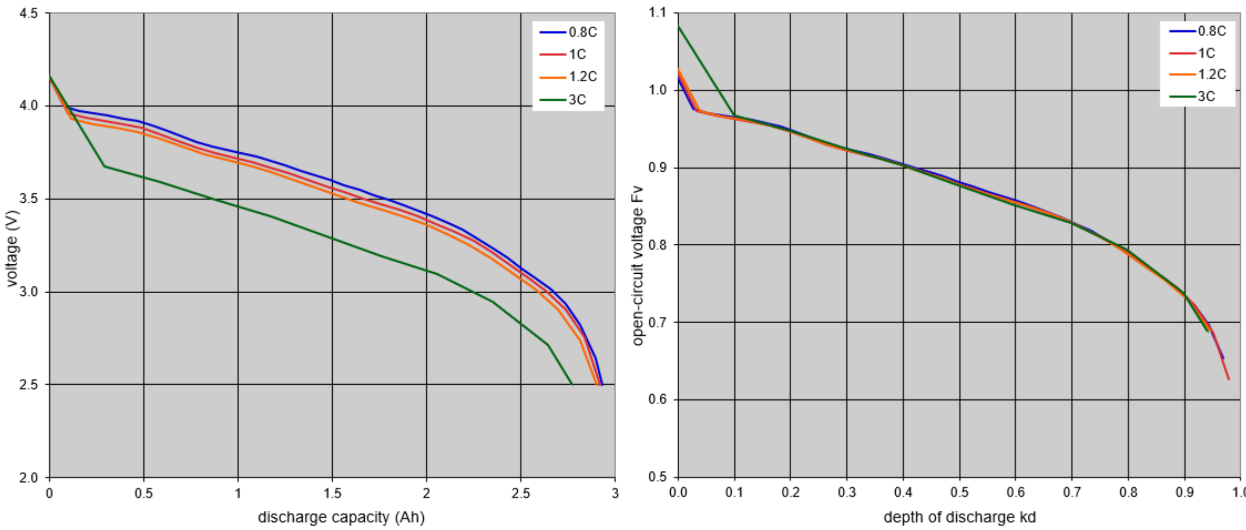


**Fig. 4 Cell discharge curves (left), and normalized curves (right).**

Like the Equivalent Circuit model, this model does not take aging or capacity fade into account. It also assumes constant internal resistance ($R$) as one of the model parameters, rather than solving for resistance dynamically.

There are some noteworthy advantages to using this type of model. The pre-configured interpolation table enables fast computational speeds with good accuracy. The model requires commonly available data such as an original equipment manufacturer (OEM) battery discharge chart, which can be reasonably guessed for notional batteries. In addition, generalized trends for the normalized data based on measurements from multiple lithium-ion batteries are available in the NDARC documentation [11].

A disadvantage of this model is that its accuracy is dependent on the amount of data provided by the user. Because parameters such as $R$ are assumed to be constant, high C-rates would not be modeled accurately if only low C-rates were provided to the model, and vice versa. Additionally, this model does not capture transient behavior of the battery, leading to larger inaccuracies immediately following changes in current.

### C. Curve Fit Model

The method applied in the EMTAT software package [12] is based on Shepherd's voltage-current model [4, 19]. The model is parameterized for a particular battery by defining a discharge curve function with exponential and nominal regions as shown in Fig. 5.

The parameters $A$, $B$, $K$, $R$, and $E_0$ shown in Eq. 6 - 10 are adjusted to best fit the provided user data, and then used to solve Shepherd's model for voltage. The parameter equations coincide with the voltage and capacity of the maximum, exponential, and nominal points, which are also adjusted to fit the provided data. The scalar values 1.4 and 0.185 in the equations for $B$ and $K$ respectively are used to improve the fit to the particular battery being modeled and can be adjusted manually by the user [19].

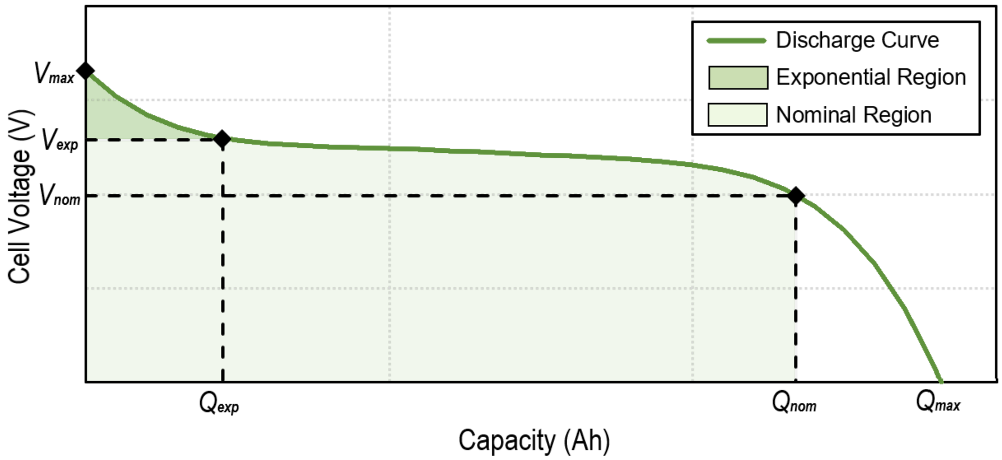


**Fig. 5 Idealized regions of battery discharge curve [19].**

$$A = V_{max} - V_{exp} \qquad B = \frac{1.4}{Q_{exp}} \qquad K = 0.185\left(V_{max} - V_{nom} + A\left(e^{-B*Q_{nom}} - 1\right)\right) * \frac{Q_{max} - Q_{nom}}{Q_{nom}}$$

$$R = V_{nom}\left(\frac{1 - \nu}{0.2 * Q_{nom}}\right) \qquad E_0 = V_{max} + K + R * I - A \tag{6, 7, 8, 9, 10}$$

Eq. 11 shows Shepherd's equation for battery voltage with variable current discharge:

$$V_{cell}(t) = E_0 - K\frac{Q_{max}}{Q_{max} - Q}(I(t) + I) - R_O * I(t) + Ae^{-B*It} \tag{11}$$

The EMTAT software contains a MATLAB user interface that allows the user to visually adjust the exponential and nominal regions as well as the parameters. The position of the regions can easily be derived from manufacturer battery specifications, allowing rough estimation of the battery's discharge curve data even when such data is not available. The MATLAB interface contains options to use RMSE or $R^2$ regression to fit the parameters to the user's data automatically if desired.

Like the other models, this model does not take aging or capacity fade into account. The model contains a few numerical assumptions not exposed to the user directly, such as the scalar values in Eqs. 7 and 8.

This approach can be beneficial in several ways. The automatic curve-fitting methods available in the EMTAT software can be used to make the setup nearly automatic for the user, requiring only discharge curve data to be provided. The model is also apt for visual representation, allowing the user to easily adjust the parameters and region locations in real time. This makes the approach well suited to sizing a notional cell for a specific operation. In addition, this model is analytic, meaning no interpolation is required. This may be desired for certain applications.

Limitations of the approach include the trial and error required from the user to accurately tune the model. The automatic curve-fitting methods are sensitive, and do not completely replicate the parameters found from fitting the curves manually. The model is somewhat limited when modeling high-capacity cells. The fitted curve shape assumes a high voltage decrease at low SOC that cannot be completely overcome by adjusting parameters, making the model somewhat inaccurate for the battery examined in this study. This could likely be overcome by altering the underlying equations of the model or by applying a correction factor.

## IV. Battery Model Comparison

### A. Experimental Validation

The Samsung INR18650-30Q battery cell is selected for model comparison, due to its commercial availability and use on existing NASA concept models [20, 21]. Previous work for the X-57 Maxwell involved testing these cells using the methods described in Section III for steady discharge currents, as well as the notional cell power load of a nominal mission [5]. Each of the examined battery models are first tuned to this test data, then compared with tested discharge curves at 0.8C, 1.0C, 1.2C, and 3C rates to determine their constant discharge performance. Next, the models are compared with the tested notional power load using time-based power inputs in MATLAB Simulink [14] to determine their variable discharge performance.

The constant discharge performance of each of the battery models is shown in Fig. 6. For clarity, only the standard (1C) and high (3C) discharge rates are shown. It should be noted that the Equivalent Circuit and Normalization models are both subject to measurement error from the cell tests. While a smoothing function can be applied to mitigate this effect in actual use, no smoothing was applied for a more direct comparison with the Curve Fit model. The variance seen in the plots is due primarily to this measurement error.

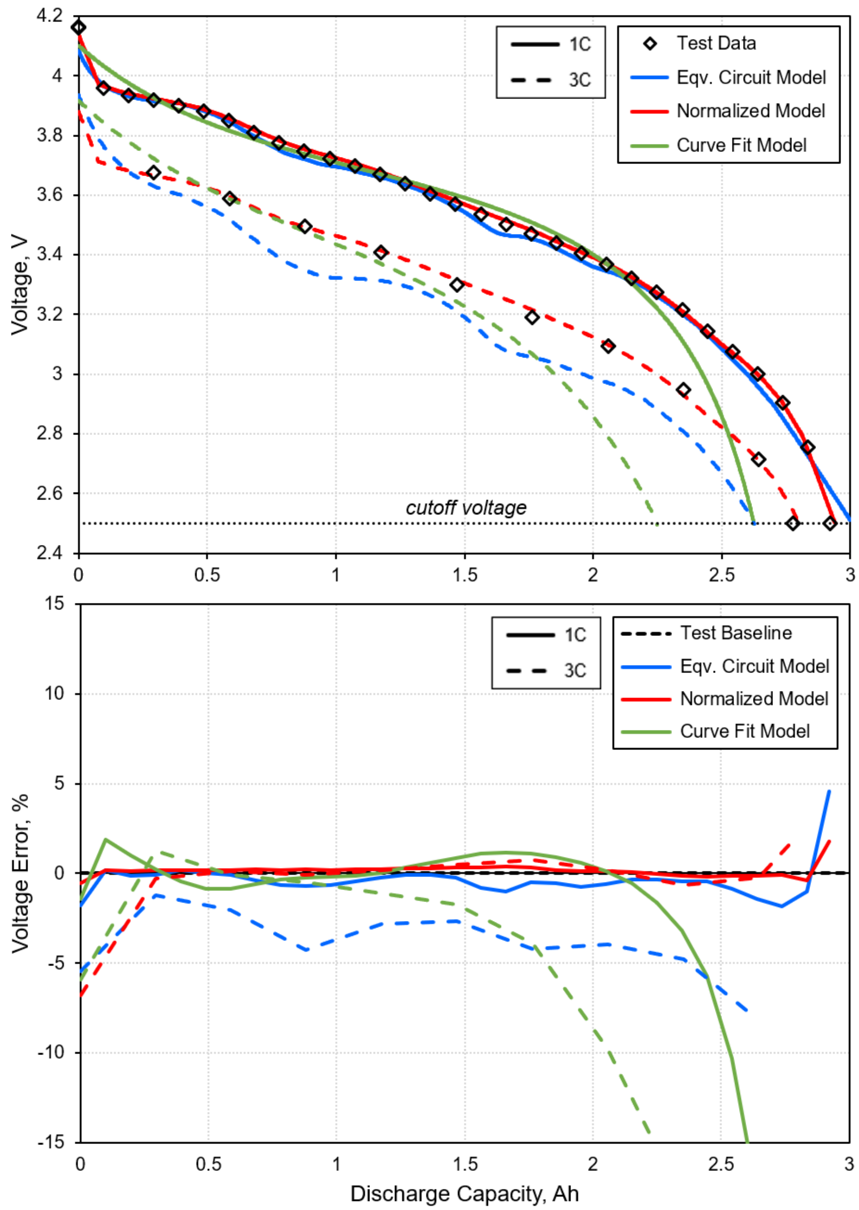


**Fig. 6 Constant discharge model cell voltages (top) and percent errors (bottom).**

The Equivalent Circuit model slightly overestimates voltage loss at a standard discharge rate, with an amplified effect at higher rates. The transient effects of the initial voltage drop are captured most accurately with this model. The Normalized model closely matches the data after the initial voltage drop. Due to challenges tuning the Curve Fit model to this type of battery cell, the model overestimates the voltage loss at low SOC.

The nominal mission power load consists of taxi, flight check, climb, cruise-climb, cruise, approach, rollout, and reserve segments for the X-57 Maxwell. The mission discharge performance for each of the battery models is shown in Fig. 7, along with a keyed guide for the duration of each flight segment.

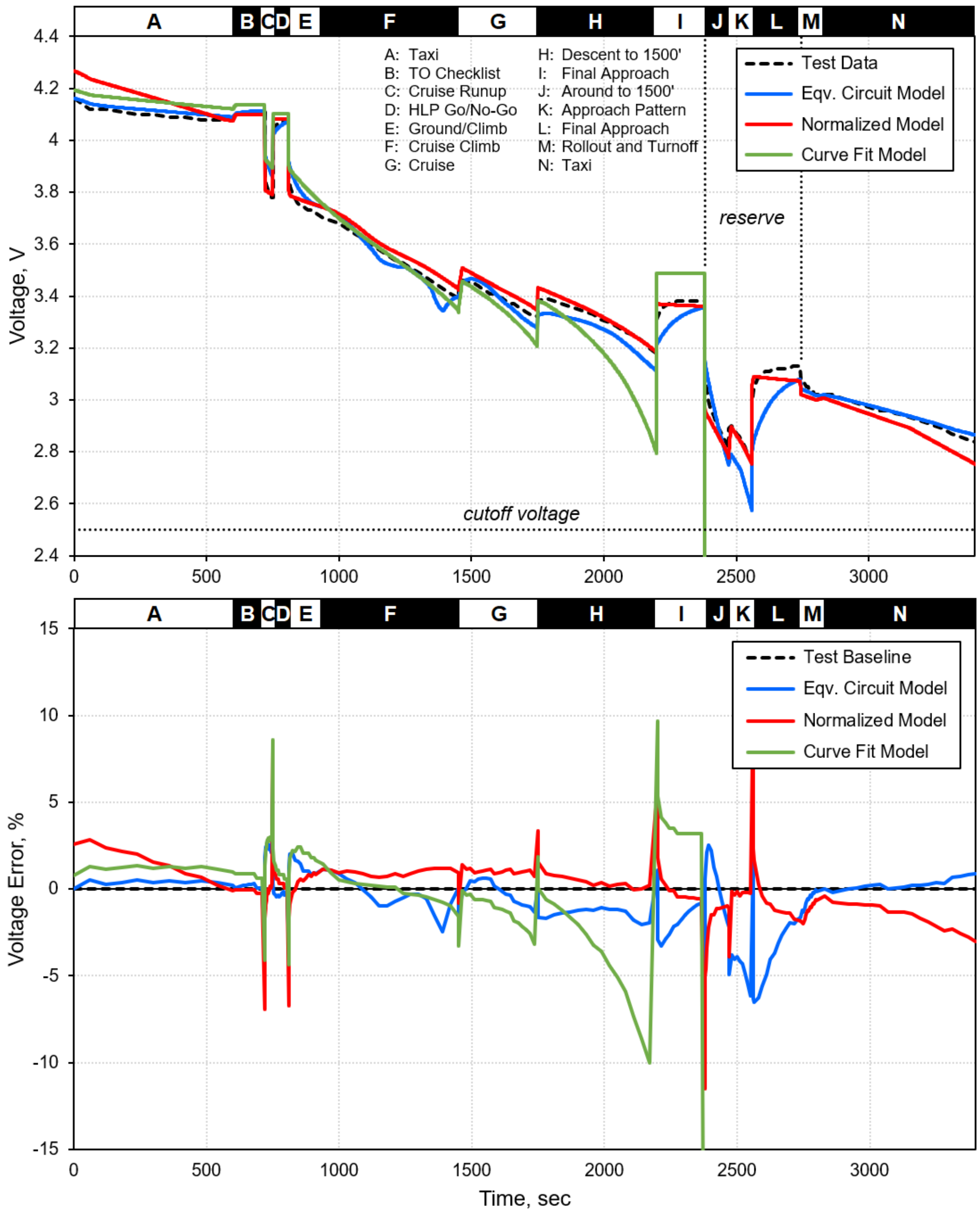


**Fig. 7 Example notional mission model cell voltages (top) and percent errors (bottom).**

Similar results to the steady discharge data can be seen, with the models overestimating voltage loss at lower SOC. Transient effects of changes in current are best captured with the Equivalent Circuit model. The Normalized model most closely matches the experimental data, but does not accurately model the initial and final low-power segments. The Curve Fit model accurately reflects the test data at high SOC, but fails to converge at low SOC due to near-zero or negative voltage values. The mean percent error (MPE) for both the steady discharge and mission validation cases are shown in Table 2 at the end of this section.

## B. Mission Definition

To determine the applicability of each battery model in a larger design context, each of the models are applied to a simple MDAO problem for NASA's Six-Passenger Quadrotor concept shown in Fig. 8. Previous studies [16, 17] identified a regional sizing mission consisting of departure and return flights of 37.5 nmi each into a 10-knot headwind with a cruise reserve of 20 minutes. The labeled sizing mission profile is shown in Fig. 9. Using the NDARC software, the predicted power load and performance of the vehicle was determined. Given the previously sized specific energy and weight of the vehicle's battery pack and the power and duration requirements of the sizing mission profile, the battery pack performance is equivalently compared between each of the battery modeling methods. Then, assuming a variable-length cruise segment, the battery modeling methods are used to optimize the battery pack series and parallel cell configuration for optimal mission range. The optimization problem is created using OpenMDAO, an open-source Python environment designed to assess and optimize multidisciplinary problems. Dymos, an optimal control library for OpenMDAO, is incorporated to allow parameterized modeling of the sizing mission using defined segments.

**Fig. 8 Rendering of NASA Six-Passenger Quadrotor Concept [17].**

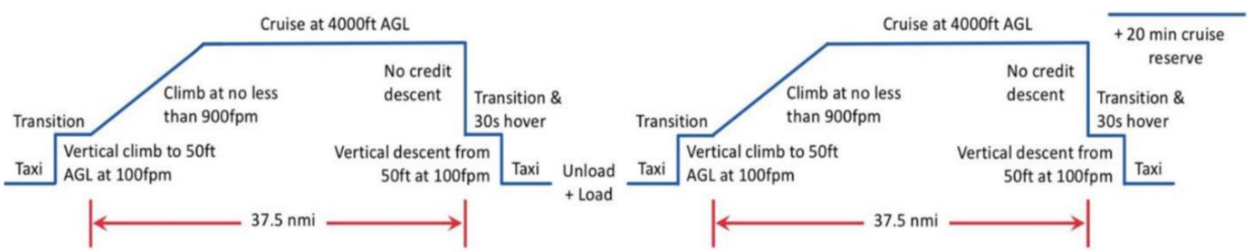


**Fig. 9 UAM vehicle-sizing mission profile [16].**

Several assumptions are made for the battery pack and powertrain for simplicity of the battery design. It is assumed the DC motors have an operating voltage of 700V with a maximum allowable bus voltage of 1000V. A simplistic battery management system (BMS) limits the SOC to a minimum of 20% and cuts off the system at minimum voltage.

A simple thermal model is applied to each of the battery models so that their performance can be measured equally. It is assumed that heat is expelled only through air convection at a constant ambient temperature. No modifier is added to the convection on the cell level to account for structure, insulation, or uneven heat flux. The cell heat is approximated from cell current and internal resistance. The temperature change is calculated from Eq. 12:

$$\frac{dT}{dt} = \frac{I^2 R_{total} - h_{cell} A_{S,cell} \Delta T}{C_{p,cell}} \tag{12}$$

As part of the EMTAT package, the Curve Fit model contains a simple heat exchanger model that draws additional power from the battery to maintain a lower temperature. This is disabled for the purpose of comparing with the other models.

A weight penalty of 30% is added to the total cell weight to account for the BMS, structure, wiring, and other weights associated with the battery pack assembly. While this is an adequate assumption for this comparison study, it should be noted that the specific energy penalty for a battery pack assembly does not scale linearly with the specific energy of the cell [22]. The 18650-30Q cells have a specific energy of about 225 Wh/kg, which is insufficient to model the UAM sizing mission which assumes a pack specific energy of 400 Wh/kg. Accounting for the SOC limit and pack weight penalty assumption, this results in a required cell specific energy of 650 Wh/kg. To model the Quadrotor in accordance with the sizing mission, the cells are modeled after the 18650-30Q data but with a specific energy of 650 Wh/kg. This is done by artificially decreasing the weight of the cells.

As discussed in Section III, it is also assumed that no effects of aging or capacity fade apply to the battery cells. A list of the battery specifications and assumptions is shown in Table 1.

**Table 1 Battery Design Specifications and Assumptions.**

| Battery Specifications / Assumptions | Quantity |
|---|---|
| Maximum Bus Voltage ($V_{dc}$) | 1000 |
| Bus Cutoff Voltage ($V_{dc}$) | 700 |
| Battery Pack Weight (kg) | 914.13 |
| Battery Pack Weight Penalty | 0.30 |
| Battery Pack Specific Energy (Wh/kg) | 400 |
| Minimum Operating SOC (%) | 20 |
| Ambient Air Temperature (deg C) | 20 |

### C. Fixed-Range Mission

To compare the battery models equally, a 27.5 nmi mission range is used. A more detailed analysis of the battery using the three models indicated a mission range less than the 37.5 nmi expected in the original mission sizing study. This is due to the voltage and current limits placed on the electrical system architecture, added heat and capacity losses, and the tendency of the battery models to overestimate voltage loss (especially the Curve Fit model, which returned a significantly decreased mission range of approximately 27.5 nmi). A battery pack configuration of 220 series and 165 parallel cells is chosen for an equal battery pack comparison. The resulting battery performance plots are shown in Figs. 10 and 11.

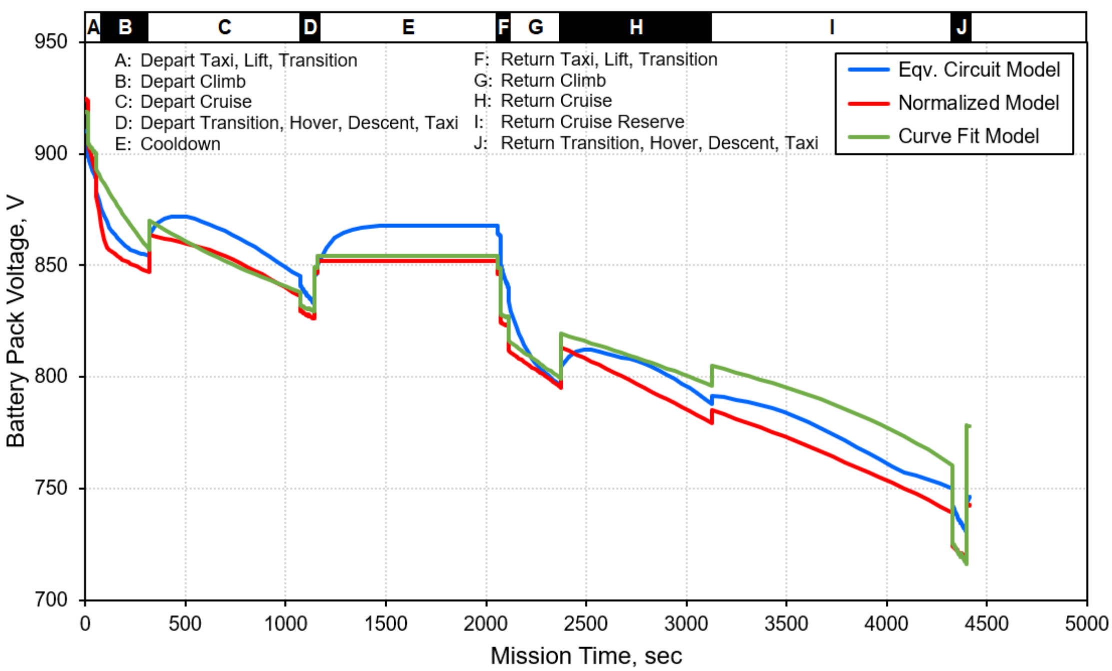


**Fig. 10 Fixed mission model battery pack voltages.**

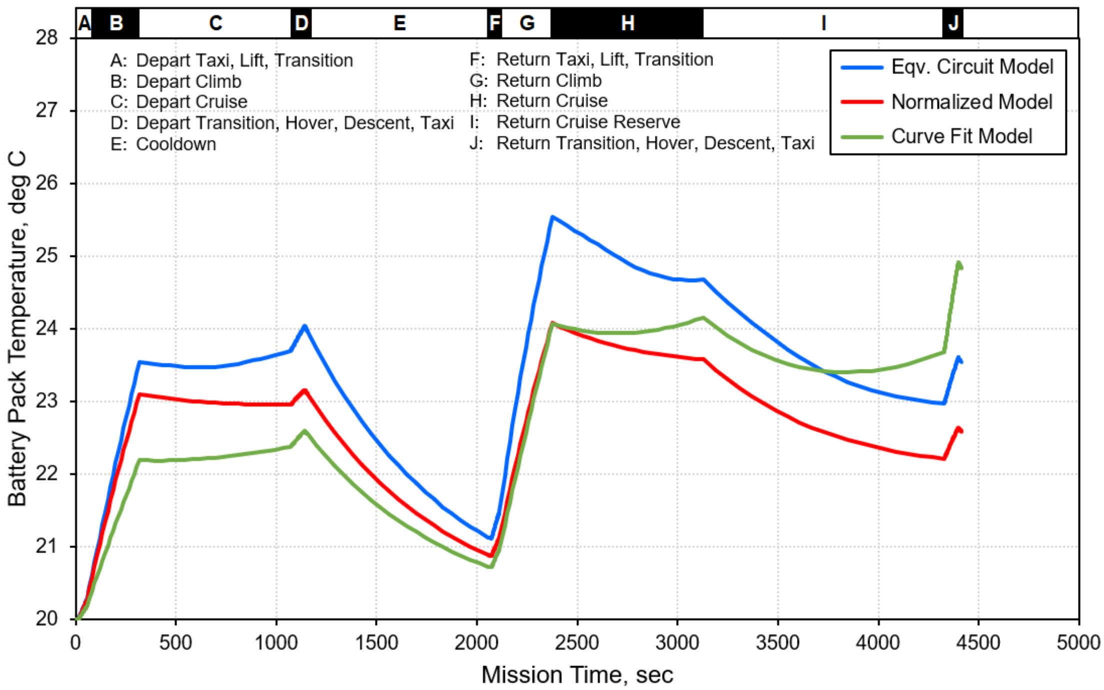


**Fig. 11 Fixed mission model battery pack net temperatures.**

With the given fixed parameters, the models remain within roughly +/- 10V throughout the mission. The Normalized and Curve Fit models do not capture the nonlinear effects from the Equivalent Circuit model, but this does not significantly deviate the overall battery performance. The temperature models remain within roughly +/- 1C, the difference being due to interpolated resistance values for the Equivalent Circuit model, and fixed resistance assumptions for the Normalized and Curve Fit models.

## D. Optimized Mission

Next, the OpenMDAO and Dymos model is used to optimize the battery pack for each of the battery models for maximum mission range, with the goal of examining the impact of the different modeling approaches on an objective. The series and parallel cell configuration of the battery packs are selected as design variables. An SLSQP optimizer and Newton solver are used to model the flight trajectory such that cutoff voltage or minimum SOC is reached at the very end of the mission. The resulting battery performance plots are shown in Fig. 12.

The battery pack configuration of the Equivalent Circuit and Normalized models are similar (approx. 220 series, 165 parallel). Due to large drops in voltage from the Curve Fit model, a higher number of series cells are needed (approx. 240 series, 150 parallel) to prevent the voltage from dropping below the 700V BMS cutoff limit. This results in similar but slightly decreased mission performance for this model, due to the lower battery capacity. The mission durations match closely for each of the optimized models, with a cruise range of approximately 31.5 nmi for the departure and return flights. The total cruise range variation between the models is approximately 0.5 nmi. This variation would be increased by the Curve Fit model if the battery pack configuration was required to closely match the other two models.

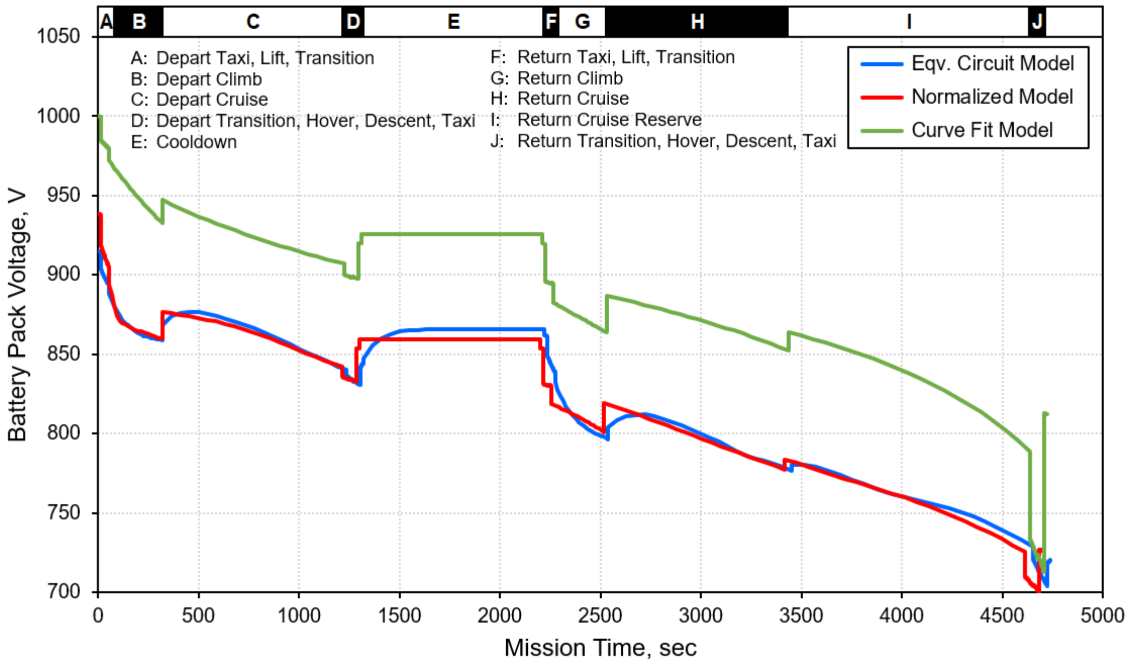


**Fig. 12 Optimized mission model battery pack voltages.**

A summary of the notable features and differences between the models is shown in Table 2. These conclusions are based on the authors' findings and may not reflect the applicability of these modeling approaches to other concept vehicles, or similar modeling approaches not discussed in this paper. Instead, these conclusions should be taken as guiding remarks on modeling approaches used by NASA's Glenn Research Center and their role in future work.

**Table 2 Battery Model Evaluation Metrics.**

| **Evaluation Metrics** | **Equivalent Circuit Model** | **Normalized Model** | **Curve Fit Model** |
|---|---|---|---|
| Optimization Computational Time (as % of fastest model): | 148% | 100% | 305% |
| Steady Discharge MPE (%): | 1.534% | 0.423% | 2.693% |
| Mission Discharge MPE (%): | 1.389% | 1.186% | 2.301% |
| Compatible Battery Types: | Power cells, energy cells | Power cells, energy cells | Power cells (may be adaptable for energy cells) |
| Data Required: | Cell specifications, pulse discharge test data | Cell specifications, OEM discharge data | Cell specifications, OEM discharge data (optional) |
| Models Charging Cycle: | No (could be added by creating a pulse charge test) | Yes | Yes |
| Captures State Transient Performance: | Yes | No | No |
| Ease of Use (not including data gathering): | Easiest | Moderate | Hardest |
| Technology Level: | Moderate Fidelity, Low Complexity | Low Fidelity, Low Complexity | Low Fidelity, Moderate Complexity |
| Compatible Battery Chemistries: | Lithium-Ion (ideally compatible with any chemistry) | Lithium-Ion | Lithium-Ion, Lead-Acid, Ni-Mh |
| Recommended Conceptual Design Situation: | Experimental Conceptual Design. Supporting test data is required. | Experimental or Notional Conceptual Design. Supporting test data is useful but not necessary. | Notional Conceptual Design. No supporting test data is required. |

## V. Conclusion

The results indicate that each of the examined models can approximate experimental battery data relatively accurately, but can be subject to net performance inaccuracy in the case of the Equivalent Circuit model or increased inaccuracy at low SOC in the case of the Curve Fit model. This has the potential to contribute significantly to mission analysis error by over-stressing the design constraints or incorrectly estimating the required electrical system architecture for the concept vehicle. This is especially true for fully electric concepts such as the examined eVTOL Quadrotor vehicle. When using these models, proper precautions must be taken and validation must be conducted to characterize model uncertainty.

Based on these findings, recommendations can be given for the best-use applications of each model in a conceptual MDAO context:

- A Thévenin Equivalent Circuit model is recommended for experimental concept design applications where cells can be physically obtained. It is also recommended for detailed cell performance analysis, such as modeling polarization discrepancies, aging, or thermal runaway, due to a more detailed ability to model transient state effects and modular precision of the circuit model.

- A Normalized model is recommended for concept design applications where OEM battery discharge data is available. It is also recommended for large multidisciplinary design problems or quick-return applications due to its accuracy and computational efficiency.

- A Curve Fit model is recommended for notional concept design applications where battery cell properties must be sized for the design rather than chosen from a selection of existing cells, or where rapid examination of different candidate cells is desired.

To meet the needs of NASA's RVLT project, future work will involve developing a Normalized model for MDAO applications outside of the NDARC software. This will help improve computational runtimes of large system models and enable the ability to examine different battery cell types more easily. Future work may also include examination of battery modeling approaches outside of those examined in this paper for additional added benefit to the project.

## Acknowledgments

The authors would like to thank the NASA Revolutionary Vertical Lift Technology (RVLT) project for support and funding for this study. The authors also thank the NASA Transformative Tools and Technologies project for funding development work that contributed to this project. The authors extend thanks to members of the Propulsion Systems Analysis branch at NASA's Glenn Research Center for their guidance.

The authors wish to thank Eliot Aretskin-Hariton for support with battery modeling in OpenMDAO. Additional thanks to Jeffrey Chin for development and support with the Equivalent Circuit Model examined in this study, and his work supporting the X-57 concept development. Thanks also to Wayne Johnson for development and support with the Normalized Model in association with the NDARC software. Finally, thanks to Mark Bell for support with the Curve Fit Model in association with the EMTAT software package.

## References

[1] Zhou, T., "Propulsive Battery Packs Sizing for Aviation Applications," Master's Thesis, Embry-Riddle Aeronautical University, Daytona Beach, Florida, May 2018.

[2] Chen, M., and Rincon-Mora, G. A., "Accurate Electrical Battery Model Capable of Predicting Runtime and I-V Performance," IEEE Transactions on Energy Conversion, Vol. 21, No. 2, pp. 504-511, June 2006, doi: 10.1109/TEC.2006.874229.

[3] He, W., Pecht, M., Flynn, D., and Dinmohammadi, F., "A Physics-Based Electrochemical Model for Lithium-Ion Battery State-of-Charge Estimation Solved by an Optimised Projection-Based Method and Moving-Window Filtering," Energies 2018, 11, 2120, doi: 10.3390/en11082120.

[4] Shepherd, C. M., "Design of Primary and Secondary Cells: II. An Equation Describing Battery Discharge," Journal of The Electrochemical Society, Vol. 112, No. 7, 1965, doi: 10.1149/1.2423659.

[5] Chin, J.C., Schnulo, S.L., Miller, T.B., Prokopius, K.P., and Gray, J.S., "Battery Performance Modeling on Maxwell X-57," AIAA Scitech Forum, San Diego, CA, 2019, doi: 10.2514/6.2019-0784, AIAA 2019-0784.

[6] Erdinc, O., Vural, B., and Uzunoglu, M., "A dynamic lithium-ion battery model considering the effects of temperature and capacity fading," International Conference on Clean Electrical Power, ICCEP, Capri, Italy, 2009, pp. 383-386, doi: 10.1109/ICCEP.2009.5212025.

[7] Sadhukhan, C., Mitra, S. K., Bhattacharyya, S., et al., "Modeling and simulation of high energy density lithium-ion battery for multiple fault detection," Scientific Reports 12, 9800, 2022, doi: 10.1038/s41598-022-13771-4

[8] Li, Y., Liu, G., Li, Z., "Numerical modeling of thermal runaway in high-energy lithium-ion battery packs induced by multipoint heating," Case Studies in Thermal Engineering, Vol. 38, 2022, ISSN 2214-157X, doi: 10.1016/j.csite.2022.102335.

[9] Yin Z., H., and Wang, L., "Application and Development Prospect of Digital Twin Technology in Aerospace," IFAC-Papers OnLine, Vol. 53, Issue 5, pp. 732-737, 2019, ISSN 2405-8963, doi: 10.1016/j.ifacol.2021.04.165.

[10] Tarhan, B., Yetik, O., and Karakoc, T. H., "Hybrid battery management system design for electric aircraft," Energy, Vol. 234, 2021, ISSN 0360-5442, doi: 10.1016/j.energy.2021.121227.

[11] Johnson, W., "NASA Design and Analysis of Rotorcraft – Theory," NASA Ames Research Center, Moffett Field, CA, NASA TP-2015-218751, Release 1.6, Feb 2012.

[12] Bell, M. E., and Litt, J. S., "An Electrical Modeling and Thermal Analysis Toolbox for Electrified Aircraft Propulsion Simulation," AIAA Propulsion and Energy Forum, 2020, doi: 10.2514/6.2020-3676.

[13] Gray, J.S., Hwang, J.T., Martins, J. R., Moore, K. T., and Naylor, B. A., "OpenMDAO: an Open-Source Framework for Multidisciplinary Design, Analysis, and Optimization," Structural and Multidisciplinary Optimization, Vol. 59, pp. 1075–1104, 2019, doi: 10.1007/s00158019-02211-z.

[14] Falck, R., Gray, J. S., Kaushik, P., Wright, T., "dymos: A Python package for optimal control of multidisciplinary systems," Journal of Open Source Software, Vol. 6, No. 59, pp. 2809, 2021, https://doi.org/10.21105/joss.02809.

[15] "Simulink User's Guide," The MathWorks Inc., Revised for Simulink 10.7 (Release 2023a), 2023, URL: https://www.mathworks.com/help/pdf_doc/simulink/simulink_ug.pdf [Accessed Dec. 2023].

[16] Silva, C., Johnson, W., Antcliff, K., and Patterson, M., "VTOL Urban Air Mobility Concept Vehicles for Technology Development," Aviation Technology, Integration, and Operations Conference, 2018, doi: 10.2514/6.2018-3847.

[17] Thomas, G., Chapman, J., Alencar, J. F., Haseeb, H., Sadey, D., and Csank, J., "Multidisciplinary Systems Analysis of a Six Passenger Quadrotor Urban Air Mobility Vehicle Powertrain," AIAA/IEEE Electric Aircraft Technologies Symposium (EATS), 2020, doi: 10.2514/6.2020-3564.

[18] Galushkin, N. E., Yazvinskaya, N. N., and Galushkin, D., N., "A Critical Review of Using the Peukert Equation and its Generalizations for Lithium-Ion Cells," Journal of The Electrochemical Society, Vol. 167, No. 12, 2020, doi: 10.1149/1945-7111/abad69.

[19] Raszmann, E., Baker, K., Shi, Y., and Christensen, D., "Modeling stationary lithium-ion batteries for optimization and predictive control," IEEE Power and Energy Conference, Champaign, IL, USA, 2017, pp. 1-7, doi: 10.1109/PECI.2017.7935755.

[20] Cinar, G., Cai, Y., Denney, R., and Dmitri, M., "Modeling and Simulation of a Parallel Hybrid Electric Regional Aircraft for the Electrified Powertrain Flight Demonstration (EPFD) Program," IEEE Transportation Electrification Conference and Expo (ITEC), 2022, doi: 10.1109/ITEC53557.2022.9813832.

[21] Schnulo, S., Chin, J., Falck, R., Gray, J., Papathakis, K., Clarke, S., Reid, N., and Borer, N., "Development of a Multi-Segment Mission Planning Tool for SCEPTOR X-57," AIAA Aviation Forum, Multidisciplinary Analysis and Optimization Conference, 2018., doi: 10.2514/6.2018-3738.

[22] Chin, J., Look, K., McNichols, E., Hall, D., Gray, J., and Schnulo, S., "Battery Cell-to-Pack Scaling Trends for Electric Aircraft," AIAA Propulsion and Energy Forum, 2021, doi: 10.2514/6.2021-3316.